Journal of Pharmaceutical and Biomedical Analysis 75 (2013) 7–17

Contents lists available at SciVerse ScienceDirect

Journal of Pharmaceutical and Biomedical Analysis

journal homepage: www.elsevier.com/locate/jpba

Proteomics-based identification of plasma biomarkers in oral squamous cell carcinoma

Chun-Liang Tung[a,b,1], Szu-Ting Lin[c,1], Hsiu-Chuan Chou[d], Yi-Wen Chen[c], Hwan-Chung Lin[e], Chung-Liang Tung[e], Kao-Jean Huang[f], Yi-Ju Chen[a], Ying-Ray Lee[g,h,**], Hong-Lin Chan[c,*]

[a] Department of Pathology, Chiayi Christian Hospital, Chiayi, Taiwan
[b] Department of Nursing, Chang Gung University of Science and Technology, Chiayi, Taiwan
[c] Institute of Bioinformatics and Structural Biology and Department of Medical Science, National Tsing Hua University, Hsinchu, Taiwan
[d] Department of Applied Science, National Hsinchu University of Education, Hsinchu, Taiwan
[e] Department of Oral and Maxillofacial Surgery, Chiayi Christian Hospital, Chiayi, Taiwan
[f] Department of Life Science and Institute of Biotechnology, National Dong Hwa University, Hualien, Taiwan
[g] Department of Medical Research, Chiayi Christian Hospital, Chiayi, Taiwan
[h] Department of Nursing, Min-Hwei College of Health Care Management, Tainan, Taiwan

ARTICLE INFO

Article history:
Received 28 August 2012
Received in revised form 9 November 2012
Accepted 10 November 2012
Available online xxx

Keywords:
Oral squamous cell carcinoma
2D-DIGE
Proteomic
Biomarker
Plasma

ABSTRACT

Oral squamous cell carcinoma (OSCC) is an aggressive cancer and its occurrence is closely related to betel nut chewing in Taiwan. However, there are few prognostic and diagnostic biomarkers for this disease especially for its association with betel nut chewing. Recent progresses in quantitative proteomics have offered opportunities to discover plasma proteins as biomarkers for tracking the progression and for understanding the molecular mechanisms of OSCC. In present study, plasma samples from OSCC patients with at least 5-year history of betel nut chewing and healthy donors were analyzed by fluorescence 2D-DIGE-based proteomic analysis. Totally, 38 proteins have been firmly identified representing 13 unique gene products. These proteins mainly function in inflammatory responses (such as fibrinogen gamma chain) and transport (Apolipoprotein A–I). Additionally, the current quantitative proteomic approach has identified numerous OSCC biomarkers including fibrinogen (alpha/beta/gamma) chain, haptoglobin, leucine-rich alpha-2-glycoprotein and ribosomal protein S6 kinase alpha-3 (RSK2) which have not been reported and may be associated with the progression and development of the disease. In summary, this study reports a comprehensive patient-based proteomic approach for the identification of potential plasma biomarkers in OSCC. The potential of utilizing these markers for screening and treating OSCC warrants further investigations.

1. Introduction

OSCC is an aggressive cancer and its occurrence is closely related to betel nut chewing [1,2]. Betel nut extract has been evidenced to be able to promote cell migration and early invasion mediated through Src kinases/Erk1/2 signaling pathway. In addition, betel nut extract may increase mitochondrial DNA (mtDNA) mutation in human oral tissues and contribute to the early stage of oral carcinogenesis [3]. The incidence rate and severity of OSCC have been gradually increasing in past 10 years. In 2010, OSCC became the fifth most common malignant cancer in Taiwan with a mortality rate at 13.31 per 100,000 persons (http://www.doh.gov.tw). Although most OSCC cases are usually diagnosed by pathological examination with guidelines proposed by the World Health Organization, the overall 5-year death rate is reaching 50% [4]. Accordingly, the biomarkers in response to betel nut chewing-associated OSCC are essential to prognosis

Abbreviations: 2-DE, two-dimensional gel electrophoresis; CCB, colloidal coomassie blue; CHAPS, 3-[(3-cholamidopropyl)dimethylammonio]-1-propanesulfonate; DIGE, differential gel electrophoresis; MALDI–TOF MS, matrix assisted laser desorption ionization-time of flight mass spectrometry; OSCC, oral squamous cell carcinoma; mtDNA, mitochondrial DNA; TCA, trichloroacetic acid.

* Corresponding author at: Institute of Bioinformatics and Structural Biology & Department of Medical Science, National Tsing Hua University, No.101, Kuang-Fu Rd. Sec.2, Hsin-chu, 30013, Taiwan. Tel.: +886 3 5742476; fax: +886 3 5715934.
** Corresponding author at: Department of Medical Research, Chiayi Christian Hosptial, No. 539, Jhongsiao Rd., Chiayi, Taiwan. Tel.: +886 5 2765041x5560; fax: +886 5 2765041x1094.
E-mail addresses: yingray.lee@gmail.com (Y.-R. Lee), hlchan@life.nthu.edu.tw (H.-L. Chan).
[1] These authors contributed equally to this work.

0731-7085/$ – see front matter © 2012 Elsevier B.V. All rights reserved.
http://dx.doi.org/10.1016/j.jpba.2012.11.017

and diagnosis of the disease. However, the pathogenesis of OSCC differs between foods, diet styles and countries. Hence, previous reports from other countries might not precisely reflect the characters of OSCC in Taiwan, where betel nut chewing is the primary epidemiological risk factor for the contribution to this disease.

Two-dimensional gel electrophoresis (2-DE) and MALDI-TOF MS have been widely used for profiling plasma proteins. And some of the nonionic and zwitterionic detergents such as thiourea and CHAPS have been introduced to increase the solubility of the plasma proteins. In addition, a significant improvement of gel-based analysis of protein quantifications and detections is the introduction of 2D-DIGE. 2D-DIGE is able to co-detect numerous samples in the same 2-DE to minimize gel-to-gel variation and compare the protein features across different gels by means of an internal fluorescent standard. This innovative technology relies on the pre-labeling of protein samples before electrophoresis with fluorescent dyes Cy2, Cy3 and Cy5 each exhibiting a distinct fluorescent wavelength to allow multiple experimental samples to include an internal standard. Thus, the samples can be simultaneously separated in one gel. The internal standard, which is a pool of an equal amount of the experimental protein samples, can facilitate the data accuracy in normalization and increase statistical confidence in relative quantity across gels [5,6].

So far, some groups have used proteomic strategy to screen OSCC markers. One of them used 4-nitroquinoline 1-oxide to induce OSCC formation in mouse model. This study indicated that haptoglobin has a great potential as a sensitive plasma biomarker for early detection of patients with OSCC [7]. Additionally, Jou et al. investigated the OSCC markers from saliva and identified salivary transferring is an early detection markers of OSCC [8]. In this study, a quantitative proteomics-based approach involving immunodepletion of high abundance proteins, 2D-DIGE analysis, and subsequent MALDI-TOF/TOF MS analysis have been performed to obtain a panel of plasma proteins, differentially expressed between OSCC patients with at least 5-year betel nut chewing history and healthy donors.

2. Materials and methods

2.1. Chemicals and reagents

Generic chemicals and albumin and IgG depletion kit were purchased from Sigma–Aldrich (St. Louis, Missouri, USA), while reagents and Cy2/Cy3/Cy5 dyes for 2D-DIGE were purchased from GE Healthcare (Uppsala, Sweden). All the chemicals and biochemicals used in this study were of analytical grade. All the primary antibodies used in this study were purchase from GeneTex (Hsinchu, Taiwan).

2.2. Plasma sample collection and purification

January 2011 to December 2011, twenty donors in a single hospital (Chiayi Christian Hospital, Chiayi, Taiwan) were enrolled in the study. Those included in the study were divided into OSCC patients ($n = 10$) and healthy donors group ($n = 10$). The criteria to assess the presence of OSCC were based on the pathological diagnosis and guidelines proposed by the World Health Organization. Healthy individuals were selected with similar age and with no OSCC diagnosed clinically. The clinical data of patients were measured in the clinical laboratory and are summarized in Table 1. This study was approved by the Institutional Research Board and carried out according to the Helsinki Declaration Principles. Written informed consent was collected from all participating subjects.

Table 1
Clinical parameters for oral squamous cell carcinoma patients participating in this study (values are mean ± SD).

	Case ($N = 10$)	Control ($N = 10$)	P-value
Sex	9 (M) + 1 (F)	7 (M) + 3 (F)	
Age (years)	50.7 ± 13	45.5 ± 7.9	0.2869
GOT ($U\,l^{-1}$)	37.7 ± 24.2	20 ± 5.6	0.0613
GPT ($U\,l^{-1}$	51.5 ± 31.6	33.4 ± 24.7	0.17
BUN ($mg\,dl^{-1}$)	13.7 ± 3.2	14.4 ± 4.4	0.6788
Creatinine ($mg\,dl^{-1}$)	1.1 ± 0.3	1.0 ± 0.2	0.2799

The values in this table are calculated with the non-parametric test. GOT: glutamate oxaloacetate transaminases; GPT: glutamic pyruvic transaminase; BUN: blood urea nitrogen.

To improve the performance of proteomic analysis of the plasma samples, the albumin and immunoglobulin G in the collected plasma samples were depleted using an albumin and IgG removal kit (Sigma–Aldrich, St. Louis, Missouri, USA) in according with the manufacturer's instructions. The depleted plasma samples were precipitated by adding 1 volume of trichloroacetic acid (TCA) (100%, −20 °C) (Sigma–Aldrich, St. Louis, Missouri, USA) to 4 volumes of sample and incubated for 10 min at 4 °C. The precipitated protein was then recovered by centrifugation at 13,000 rpm for 10 min, and the resulting pellet was washed twice with ice-cold acetone. Air-dried pellets were resuspended in 2-DE lysis buffer containing 3-[(3-cholamidopropyl)dimethylammonio]-1-propanesulfonate (CHAPS) (4%, w/v), urea (7 M), thiourea (2 M), Tris–HCl (pH8.3, 10 mM), EDTA (1 mM) (Sigma–Aldrich, St. Louis, Missouri, USA).

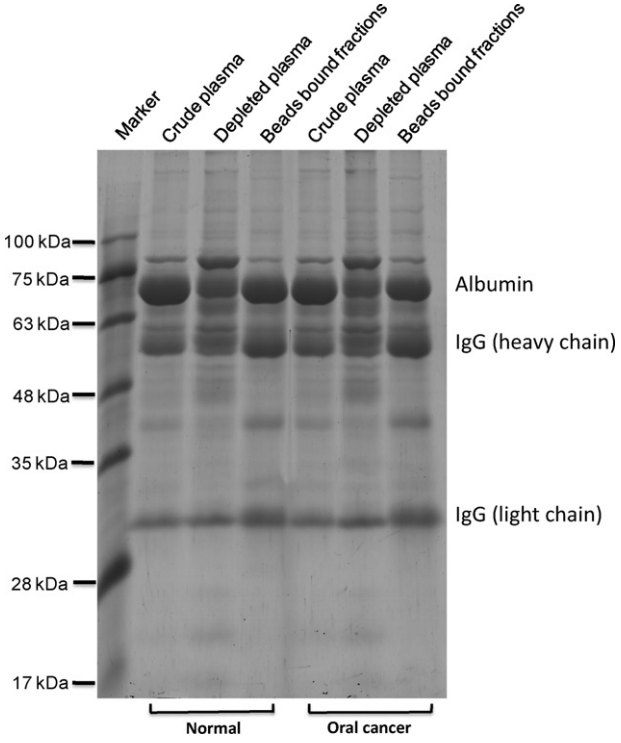

Fig. 1. The efficiency evaluation for removal of albumin and immunoglobulin G from plasma samples. 20 μg of the crude plasma, albumin and immunoglobulin-depleted plasma and beads bound protein fractions from healthy donors and OSCC patients were loaded and resolved by SDS-PAGE followed by stained with colloidal coomassie blue G-250.

A

	Cy2 (100 μg)	Cy3 (100 μg)	Cy5 (100 μg)
Gel 1	Pool	Normal	Oral cancer
Gel 2	Pool	Oral cancer	Normal
Gel 3	Pool	Normal	Oral cancer

B

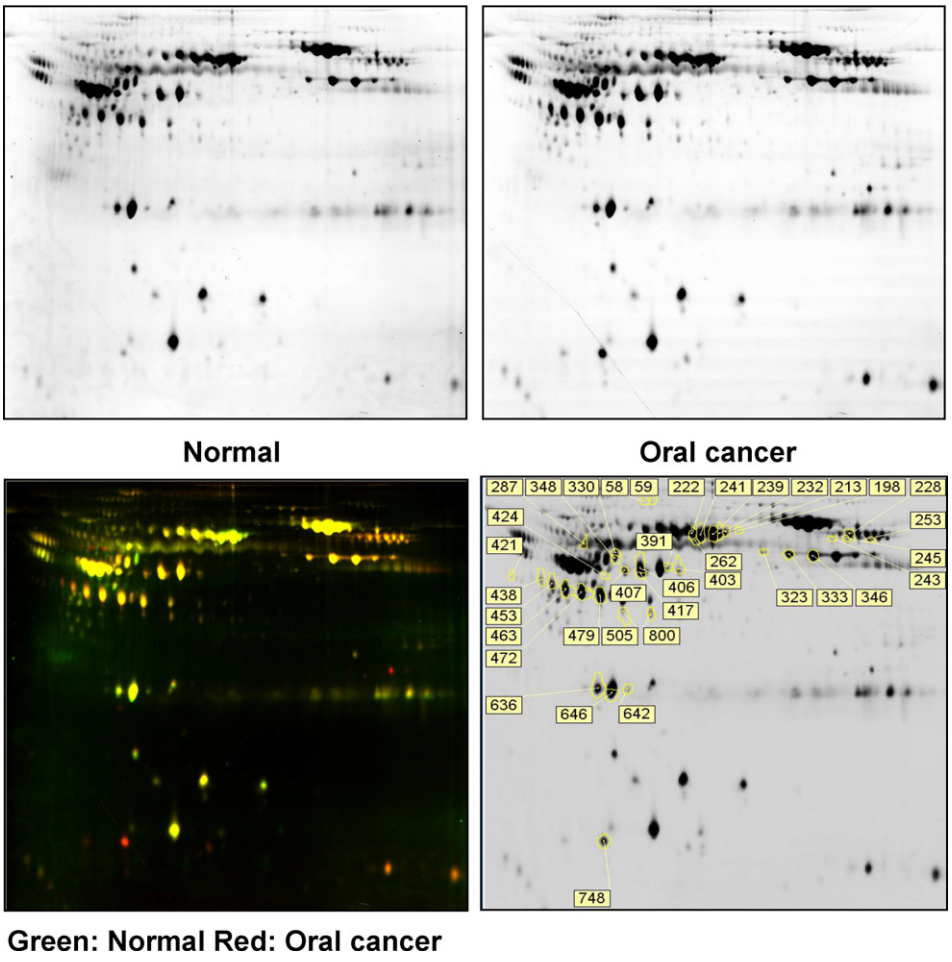

Fig. 2. 2D-DIGE analysis of OSCC-induced differentially expressed proteins. (A) Plasma samples arrangement for a triplicate 2D-DIGE experiment. (B) Plasma samples (100 μg each) were labeled with Cy-dyes. 2D-DIGE images of the plasma samples from OSCC patients and healthy individuals at appropriate excitation and emission wavelengths were shown (upper images) as well as overlaid pseudo-colored image processed with ImageQuant Tool (GE Healthcare) (left bottom). The differentially expressed identified protein features are annotated with spot numbers (right bottom).

2.3. Sample preparation for 2D-DIGE and gel image analysis

The procedure for sample preparation and Cy-dyes labeling for 2D-DIGE analysis were performed according to the previous work with some modifications [9]. Briefly, the plasma protein pellets were dissolved in 2-DE lysis buffer and protein concentrations were determined using coomassie protein assay reagent (BioRad, Hercules, California, USA). Before performing 2D-DIGE, plasma samples from 10 OSCC patients and 10 healthy donors were pooled, individually. 100 μg of protein samples from patients and healthy donors were labeled with 250 pmol of either Cy3 (GE Healthcare, Uppsala, Sweden) or Cy5 (GE Healthcare, Uppsala, Sweden) for triplicate comparison on three 2-DE, respectively. To facilitate image matching and cross-gel statistical comparison, a pool of all samples was also prepared and labeled with Cy2 (GE Healthcare, Uppsala, Sweden) at a molar ratio of 2.5 pmol Cy2/μg of protein as an internal standard for all gels. Thus, the triplicate samples and the internal standard could be run and quantify on multiple 2-DE. The detailed procedures for fluorescence dye-labeling, isoelectric focusing electrophoresis, two-dimensional electrophoresis, fluorescence image detection/analysis were described in the previous publication [10]. Spots displaying in all of 9 gel images (3 images per gel) with a $\geq$1.3 average-fold increase or decrease in abundance and a p-value < 0.05 were selected for protein identification.

2.4. Protein staining, in-gel digestion and MALDI–TOF MS analysis

Colloidal coomassie blue G-250 staining was used to visualize CyDye-labeled protein features in 2-DE followed by excised interested post-stained gel pieces for MALDI–TOF MS (Bruker Daltonics,

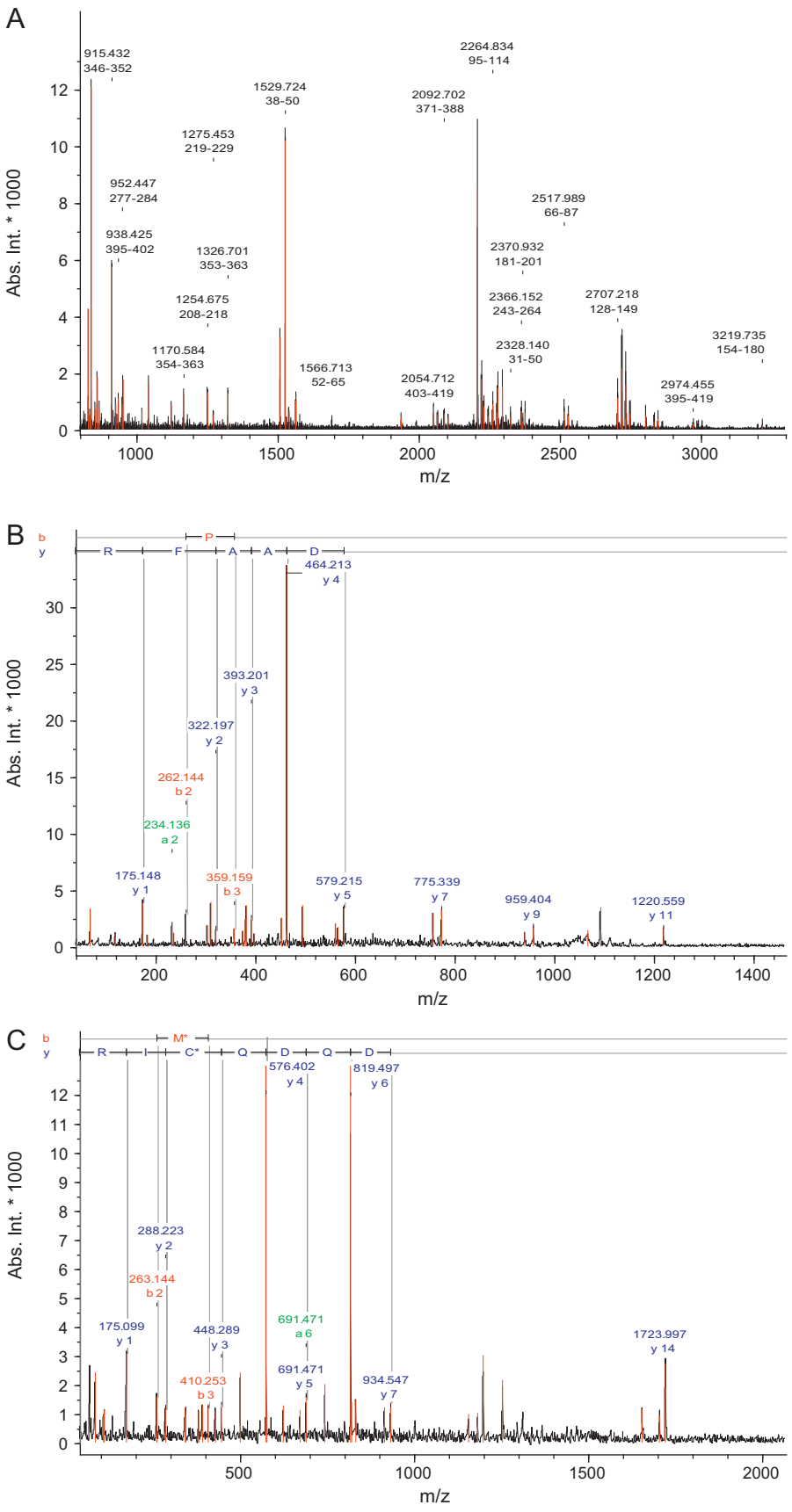

Fig. 3. Protein identification by mass spectrometry. (A) Vitamin D-binding protein was resolved by MALDI–TOF MS; (B) hemopexin and (C) haptoglobin were resolved with MALDI–TOF MS/MS.

Table 2
Alphabetical list of differentially expressed plasma proteins between OSCC patients and healthy individuals as identified by MALDI–TOF MS and MS/MS after 2D-DIGE analysis.

Spot No.	Accession No.	Protein name	pI	MW	Match. Peptides	Cov. (%)	Score	Oral cancer/ Normal[b]	*P*-value	Subcellular location	Function	Matched peptides
59	Q86XL3	Ankyrin repeat and LEM domain-containing protein 2	6.66	104,905	8/17	7%	60/56	1.36	0.007	Membrane	Unknown	TPEDVICER; HEDQLEVTR
198	Q86XL3	Ankyrin repeat and LEM domain-containing protein 2	6.66	104,905	8/14	7%	66/56	−1.6	0.0044	Membrane	Unknown	TPEDVICER; HEDQLEVTR
636	P02647	Apolipoprotein A–I	5.56	30,759	9/28	29%	90/56	−1.4	0.0025	Secreted	Transport	VQPYLDDFQK; THLAPYSDELR
642	P02647	Apolipoprotein A–I	5.56	30,759	8/39	32%	95/56	−1.38	0.0097	Secreted	Transport	DYVSQFEGSALGK; LSPLGEEMR
646	P02647	Apolipoprotein A–I	5.56	30,759	8/32	32%	77/56	−1.37	0.026	Secreted	Transport	WQEEMELYR; THLAPYSDELR
642	P02647	Apolipoprotein A–I[a]	5.56	30,759	1/1	4%	68/56	−1.38	0.0097	Secreted	Transport	THLAPYSDELR
424	Q15024	Exosome complex component RRP42	5.08	32,428	5/19	21%	65/56	−1.92	0.045	Nucleus	RNA process	VYIVHGVQEDLR; EESLGPKR
228	P02671	Fibrinogen alpha chain	5.70	95,656	9/18	11%	70/56	1.35	0.024	Secreted	Inflammatory response	DRQHLPLIK; QFTSSTSYNR
243	P02671	Fibrinogen alpha chain	5.70	95,656	8/33	13%	78/56	1.37	0.016	Secreted	Inflammatory response	MKPVPDLVPGNFK; NPSSAGSWNSGSSGPGSTGNR
245	P02671	Fibrinogen alpha chain	5.70	95,656	13/46	17%	64/56	1.52	0.047	Secreted	Inflammatory response	DSHSLTTNIMEILR; MKPVPDLVPGNFK
253	P02671	Fibrinogen alpha chain	5.70	95,656	10/26	13%	75/56	1.33	0.025	Secreted	Inflammatory response	QFTSSTSYNR; GDFSSANNR
58	P02675	Fibrinogen beta chain	8.54	56,577	8/29	17%	99/56	1.73	0.0077	Secreted	Inflammatory response	QDGSVDFGR; IRPFFPQQ
333	P02675	Fibrinogen beta chain	8.54	56,577	17/52	34%	149/56	1.41	0.0027	Secreted	Inflammatory response	LESDVSAQMEYCR; QGFGNVATNTDGK
323	P02675	Fibrinogen beta chain	8.54	56,577	9/23	15%	83/56	1.46	0.023	Secreted	Inflammatory response	QDGSVDFGR; IRPFFPQQ
346	P02675	Fibrinogen beta chain	8.54	56,577	11/23	27%	117/56	1.38	0.0061	Secreted	Inflammatory response	CHAANPNGR; EDGGGWWYNR
391	Q9UC63	Fibrinogen gamma chain	5.37	52,106	11/19	27%	136/56	1.37	0.032	Secreted	Inflammatory response	QSGLYFIKPLK; VELEDWNGR
403	Q9UC63	Fibrinogen gamma chain	5.37	52,106	6/14	14%	68/56	1.31	0.006	Secreted	Inflammatory response	TSEVKQLIK; VGPEADKYR
406	Q9UC63	Fibrinogen gamma chain	5.37	52,106	21/51	57%	228/56	1.45	0.0059	Secreted	Inflammatory response	YEASILTHDSSIR; TSTADYAMFK
407	Q9UC63	Fibrinogen gamma chain	5.37	52,106	7/17	17%	88/56	1.49	0.0021	Secreted	Inflammatory response	DNCCILDER; VELEDWNGR
417	Q9UC63	Fibrinogen gamma chain	5.37	52,106	9/19	22%	105/56	1.35	0.0019	Secreted	Inflammatory response	RLDGSVDFK; VGPEADKYR
406	Q9UC63	Fibrinogen gamma chain[a]	5.37	52,106	1/1	1%	69/56	1.45	0.0059	Secreted	Inflammatory response	VELEDWNGR
438	P00738	Haptoglobin	6.13	45,861	7/37	16%	72/56	1.78	0.00062	Secreted	Inflammatory response	YVMLPVADQDQCIR; VTSIQDWVQK
453	P00738	Haptoglobin	6.13	45,861	7/22	14%	66/56	1.76	0.0000068	Secreted	Inflammatory response	SCAVAEYGVYVK; VTSIQDWVQK

Table 2 (*Continued*)

Spot No.	Accession No.	Protein name	pI	MW	Match. Peptides	Cov. (%)	Score	Oral cancer/ Normal[b]	*P*-value	Subcellular location	Function	Matched peptides
463	P00738	Haptoglobin	6.13	45,861	7/23	16%	69/56	1.55	0.0023	Secreted	Inflammatory response	VTSIQDWVQK; VGYVSGWGR
472	P00738	Haptoglobin	6.13	45,861	6/23	13%	75/56	1.46	0.00035	Secreted	Inflammatory response	GSFPWQAK; VGYVSGWGR
479	P00738	Haptoglobin	6.13	45,861	12/56	27%	96/56	1.37	0.00029	Secreted	Inflammatory response	LRTEGDGVYTLNNEK; HYEGSTVPEK
505	P00738	Haptoglobin	6.13	45,861	10/37	23%	97/56	1.54	0.0018	Secreted	Inflammatory response	YVMLPVADQDQCIR; VTSIQDWVQK
800	P00738	Haptoglobin	6.13	45,861	9/19	21%	104/56	1.54	0.0038	Secreted	Inflammatory response	GSFPWQAK; VGYVSGWGR
453	P00738	Haptoglobin[a]	6.13	45,861	1/1	3%	63/56	1.76	0.0000068	Secreted	Inflammatory response	YVMLPVADQDQCIR
222	P02790	Hemopexin	6.55	52,385	8/27	18%	77/56	−1.4	0.023	Secreted	Transport	NFPSPVDAAFR; FDPVRGEVPPR
262	P02790	Hemopexin	6.55	52,385	10/20	23%	115/56	−1.43	0.0044	Secreted	Transport	NFPSPVDAAFR; FDPVRGEVPPR
262	P02790	Hemopexin[a]	6.55	52,385	1/1	2%	83/56	−1.43	0.0044	Secreted	Transport	NFPSPVDAAFR
287	P01877	Ig alpha-2 chain C region	5.71	37,301	5/18	12%	61/56	1.59	0.028	Membrane	Immune response	WLQGSQELPR; SAVQGPPER
421	P02750	Leucine-rich alpha-2-glycoprotein/LRG1	6.45	38,382	5/16	12%	67/56	1.33	0.034	Secreted	Inflammatory response	ALGHLDLSGNR; VAAGAFQGLR
748	P51812	RSK2/Ribosomal protein S6 kinase alpha-3	6.41	84,025	7/17	10%	61/56	4.35	0.0000026	cytosol	Signal transduction	LYLILDFLR; KETMTMILK
213	Q9P157	Serum albumin	5.92	71,317	8/18	10%	76/56	−1.81	0.0021	Secreted	Transport	HPDYSVVLLLR; KYLYEIAR
232	Q9P157	Serum albumin	5.92	71,317	9/17	11%	99/56	−1.83	0.016	Secreted	Transport	RHPDYSVVLLLR; HPDYSVVLLLR
239	Q9P157	Serum albumin	5.92	71,317	14/27	21%	138/56	−1.84	0.0091	Secreted	Transport	RHPDYSVVLLLR; HPDYSVVLLLR
241	Q9P157	Serum albumin	5.92	71,317	8/15	10%	84/56	−1.76	0.0021	Secreted	Transport	RHPDYSVVLLLR; HPDYSVVLLLR
330	P02774	Vitamin D-binding protein	5.40	54,526	19/53	54%	185/56	−1.89	0.013	Secreted	Transport	FPSGTFEQVSQLVK; THLPEVFLSK
348	P02774	Vitamin D-binding protein	5.40	54,526	6/18	10%	67/56	−2.16	0.00056	Secreted	Transport	HLSLLTTLSNR; RTHLPEVFLSK

[a] Proteins identified by MALDI–TOF/TOF.

[b] Average fold-differences of triplicate samples run on different gels from DeCyder analysis show abundance ratios for OSCC patient's plasma versus healthy donor's plasma.

Bremen, Germany) identification. The detailed procedures for protein staining, in-gel digestion, MALDI–TOF MS analysis and the algorithm used for data processing were described in the previous publication [10]. The spectrometer was also calibrated with a peptide calibration standard (Bruker Daltonics, Bremen, Germany) and internal calibration was performed using trypsin autolysis peaks at m/z 842.51 and m/z 2211.10. Peaks in the mass range of m/z 700–3000 were used to generate a peptide mass fingerprint that was searched against the Swiss-Prot/TrEMBL database (release on 2011_08) with 531473 entries using Mascot software v2.3.02 (Matrix Science, London, UK). The following parameters were used for the search: *Homo sapiens*; tryptic digest with a maximum of 1 missed cleavage; carbamidomethylation of cysteine, partial protein N-terminal acetylation, partial methionine oxidation and partial modification of glutamine to pyroglutamate and a mass tolerance of 50 ppm. Identification was accepted based on significant MASCOT Mowse scores ($p < 0.05$), spectrum annotation and observed versus expected molecular weight and pI on 2-DE.

2.5. Immunoblotting analysis and ELISA analysis

Immunoblotting and ELISA analysis were used to validate the differential abundance of mass spectrometry identified proteins. The detailed experimental procedures were described in the previous reports [11]. All of primary antibodies used for expression validation were purchased from Genetex (Hsinchu, Taiwan).

3. Results and discussion

3.1. 2D-DIGE and mass spectrometry analysis of the immunodepleted plasma proteome

The isolation of low-abundance proteins from human plasma is frequently difficult due to the existing of high abundance proteins such as serum albumin and immunoglobulin G. Immunoglobulin G and Serum albumin are the most (50–70%) and second (10–20%) abundant protein in plasma, respectively. These proteins are able to mask the low-abundant proteins and limit the amount of the total plasma proteins that can be applied and resolved by proteomic analysis. To removal of these two primary high-abundant proteins, this experiment used albumin and IgG depletion kit from Sigma–Aldrich, which contains prepacked spin columns allows removal of the most of both immunoglobulin G and serum albumin. Subsequently, this study used TCA/acetone to precipitate, desalt and enrich the plasma proteins to make them well resolved by 2D-DIGE. The current results demonstrated that this strategy did remove around 70% of serum albumin; however, this strategy did not make significant effects on removal of the light- and heavy-chains of immunoglobulin G in this depleted experiment (Fig. 1).

In order to study the alteration of plasma protein in the OSCC patients, comparative proteomics analysis was performed between OSCC patients and healthy donors. The 2-DE images of the samples of two groups were minimally labeled with Cy3 and Cy5 dyes and distributed to each gel. A pool of both samples was also prepared for labeling with Cy2 as an internal standard to run on all gels to facilitate image matching across gels (Fig. 2). The plasma samples arrangement for a triplicate 2D-DIGE experiment is shown in Fig. 2A. Thus, the triplicate samples resolved in different gels can be quantitatively analyzed by means of the internal standard on multiple 2-DE. After resolving protein samples with 2D-DIGE technique, the DeCyder image analysis software indicated that 48 protein features were showing greater than 1.3-fold change in expression level with Student's t-test (p-value) less than 0.05. MALDI–TOF MS and MS/MS identification revealed that 38 proteins (corresponding to 13 unique proteins) were differentially expressed (Figs. 2B and 3 and Table 2). Most of these identified proteins are functionally involved in inflammatory responses (57%) and transport (32%) and almost 90% of the differentially expressed proteins identified were secreted proteins (Fig. 4). Of these, plasma fibrinogen isoforms (alpha/beta/gamma) have been reported as OSCC markers in previous studies. In contrast, RSK2, leucine-rich alpha-2-glycoprotein and hapatoglobin have not been reported as OSCC markers. Further investigation indicated that the combination of these identified proteins have not yet been described as cancer markers in other cancer types. Accordingly, the combination of these identified proteins might be further evaluated as OSCC specific markers.

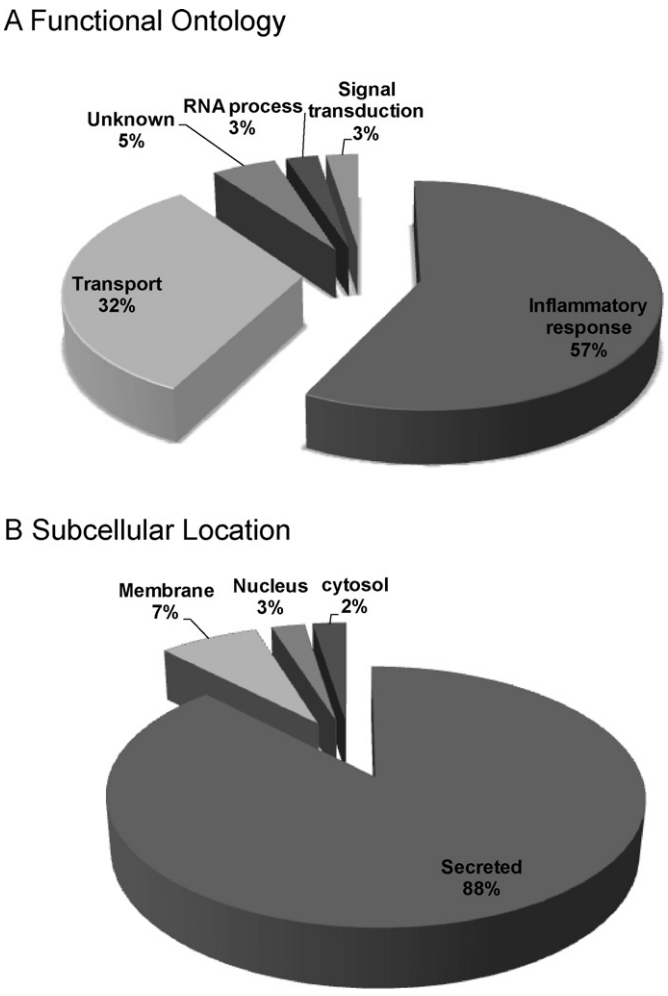

Fig. 4. Percentage of plasma proteins identified from albumin and imunnoglobulin G depleted plasma by 2D-DIGE/MALDI–TOF MS for OSCC according to their biological functions (A) and subcellular location (B).

Apolipoprotein A–I is a constituent of the high density lipoprotein responsible for the cholesterol transport in serum with a final destination in the liver. In numerous tumors such as cholangiocarcinoma, oesophageal cancer, bladder cancer, colon cancer and ovarian cancer, the apolipoprotein A–I levels are all up-regulated [12]; however, reduced plasma apolipoprotein A–I level has been reported in gastric tumor [13]. This current 2D-DIGE analysis revealed apolipoprotein A–I level is down-regulated in OSCC. These previous studies and the current result demonstrated that the regulation of apolipoprotein A–I level during tumorigenesis is complicated and needs to further clarification.

Plasma fibrinogen is a regulator during blood coagulation and has been recognized as an angiogenic and a metastatic predictor in numerous tumors; meanwhile, it is a potential indicator for malignant tumors [14]. Since OSCC is an aggressive cancer, the high

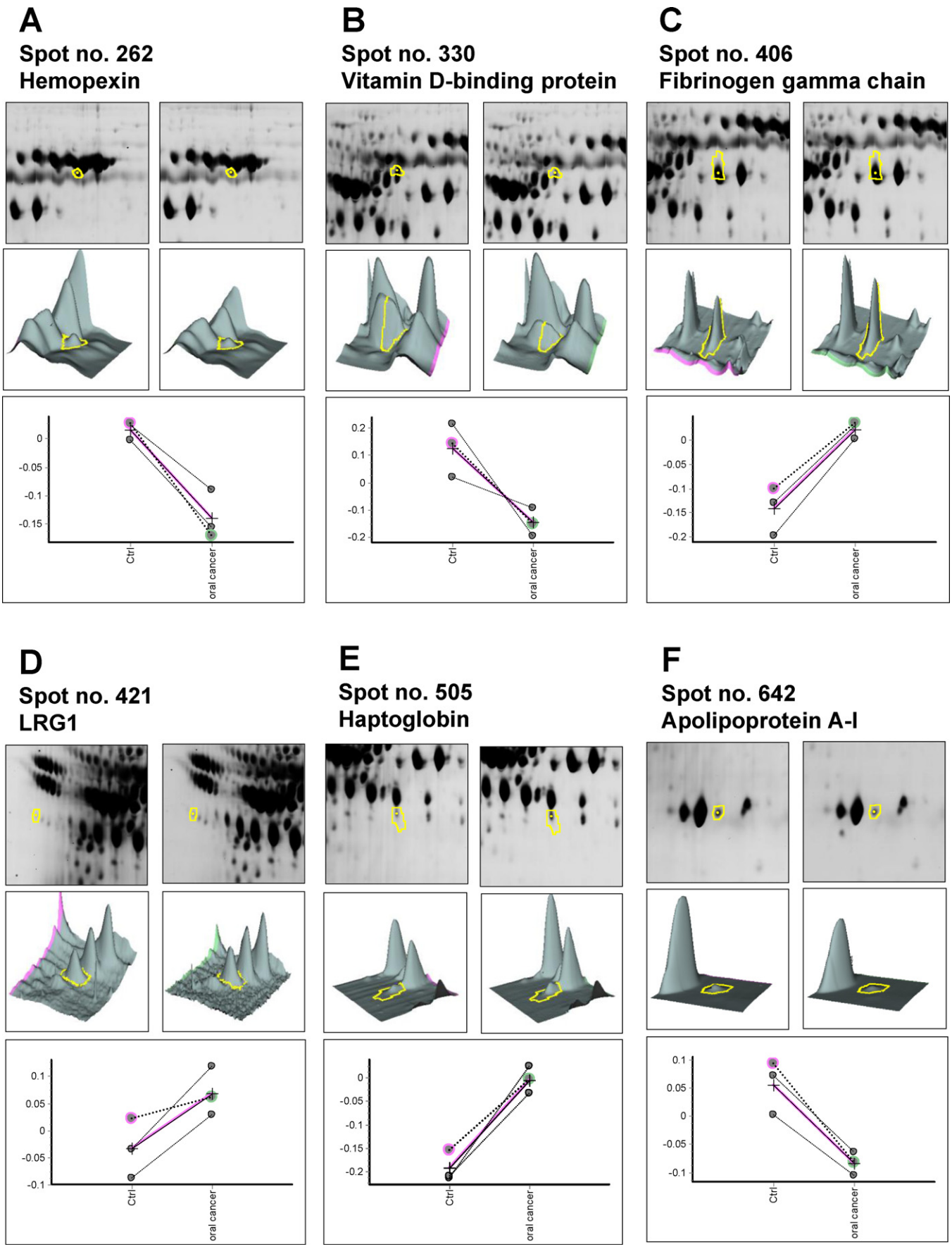

Fig. 5. Representative images of the identified spots ((A) hemopexin; (B) vitamin D-binding protein; (C) fibrinogen gamma chain; (D) leucine-rich alpha-2-glycoprotein; (E) haptoglobin; (F) apolipoprotein A–I) displaying OSCC-dependent protein abundance changes. The levels of these proteins were visualized by fluorescence 2-DE images (top panels), three-dimensional spot images (middle panels) and protein abundance map (bottom panels).

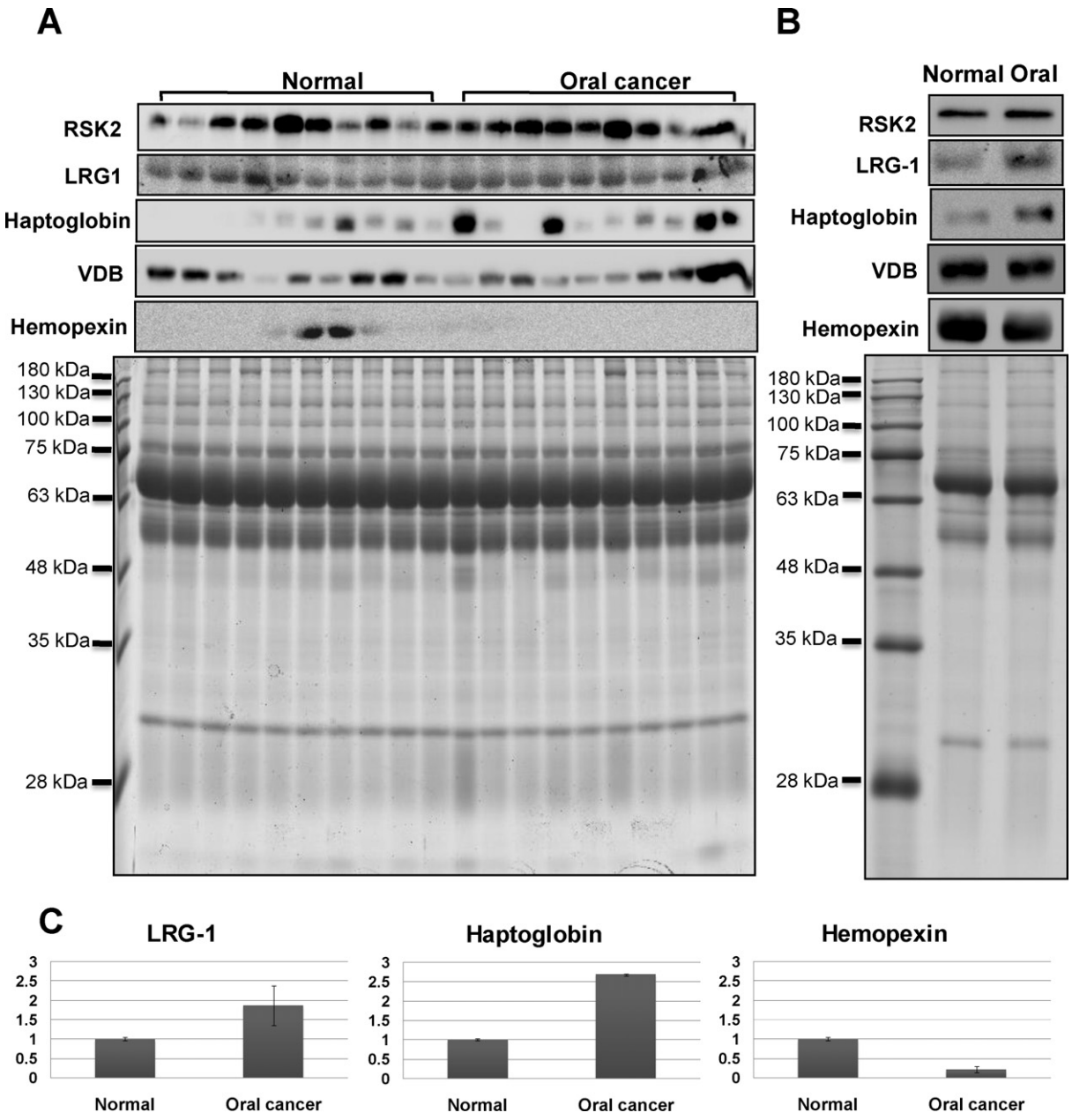

Fig. 6. Representative immunoblotting and ELISA analysis of RSK2, leucine-rich alpha-2-glycoprotein, hapatoglobin, vitamin D-binding protein, hemopexin for selected differentially expressed plasma proteins identified by proteomic analysis in patients with and without OSCC. 20 μg of the albumin and immunoglobulin-depleted plasma samples from 10 healthy donors and 10 OSCC patients were either run individually (A) or run in a pool (B). (C) 50 μg of plasma samples were coated onto each well of 96-well plate for ELISA analysis and the absorbance was measured at 450 nm using Stat Fax 2100 microtiterplate reader (Awareness Technology, Palm city, Florida, USA).

expression level of serum fibrinogen is reasonable to be observed in OSCC patients.

Leucine-rich alpha-2-glycoprotein has been shown to be involved in cell adhesion and has been evidenced to be a biomarker for certain diseases including microbial infections, ovarian cancer, non-small cell lung cancer and pancreatic cancer [15]. The current result is the first time to support leucine-rich alpha-2-glycoprotein as a plasma biomarker for OSCC.

RSK2 is one of Ser/Thr kinase family members playing essential roles in a number of cellular functions including cell survival, cell cycle and cell proliferation. Recent advances in tumor biology demonstrate a crucial role of RSK2 in tumor metastasis and progression, making RSK2 a potential therapeutic target in cancer treatment [16]. In addition, betel nut extract has been evidenced to be able to promote cell migration and early invasion mediated through Src kinases/Erk1/2 signaling pathway [17,18]. Further study suggests that Src-dependent phosphorylation at Tyr-529 facilitates RSK2 activation through Erk1/2 pathway [19]. Accordingly, these previous studies offer an explanation to show how the betel nut chewing induces OSCC as well as increases RSK2 level in patient's plasma. In the view of cancer biomarker, RSK2 has been reported to be activated in myeloid leukemia [20] and prostate cancer [21]. However, no literature reports the role of RSK2 on OSCC as well as utilizes it as a plasma cancer biomarker yet. Thus, the current result is the first time to support RSK2 as a plasma biomarker for OSCC.

Vitamin D-binding protein is a secreted transport protein which transports the vitamin D sterols in serum and prevents polymerization of actin. In clinical investigation, vitamin D-binding protein has been widely used as a biomarker for breast cancer, thyroid

cancer and lung cancer [22]. In oral cancer studies, vitamin D-binding protein has been evidenced to be elevated in mouse plasma but no evidence in human plasma [23]. This plasma proteomic analysis indicated that vitamin D-binding protein is reduced in OSCC plasma implying the disease might have differentially regulatory mechanism between human and mouse. In addition, the local diet style of betel nut chewing might also play roles in modulating plasma vitamin D-binding protein level renders further investigation.

In current study, 2D-DIGE experiment is based on fluorescence-based protein quantification which can detect sub-nanogram leve of dye-labeled proteins; however, the current post-staining experiment is based on modified colloidal coomassie blue staining with sensitivity around 10–50 ng [24]. Consequently, numerous differentially expressed dye-labeled low-abundant plasma proteins can be imaged by fluorescent scanner but failed to be visualized with colloidal coomassie blue staining. This is the reason why only 42 of 48 differentially expressed features on 2-DE can be picked for MALDI–TOF identification. Additionally, the plasma proteins are largely modified with glycans in circulation system. The high level of glycosylation on plasma proteins have been reported to interfere trypsin digestion and MALDI–TOF MS analysis [25]. Accordingly, glycosylation of plasma proteins might contribute to failure identification in this study.

Of the protein isoforms resolved and identified by 2D-DIGE and MALDI–TOF MS methods, ankyrin repeat and LEM domain-containing protein 2 was identified as doublet spots with differing pIs by lysine labeling. Notably, the more basic spot (spot 198) in the doublet was shown to be down-regulated, whilst the more acidic spot (spot 59) was up-regulated. A similar observation has been reported [26,27] and was found to be due to oxidation of the active site cysteine thiols of these proteins. Such shifts provide an explanation for the observation demonstrating that part of ankyrin repeat and LEM domain-containing protein 2 might be modified and induced a possible pI shift-induced differential labeling such as modified by the oxidation of thiol cysteines or glycosylation of the protein. This model can also be further validated by 2D-immunoblotting and the molecular modifications on ankyrin repeat and LEM domain-containing protein 2 may affect protein activity and warrant further investigation.

Representative examples for the evaluation by DeCyder of alteration in spot intensities using the 2D-DIGE system are displayed in Fig. 5. To display visually alterations in corresponding spot intensity proportions, selected identified spots (hemopexin, vitamin D-binding protein, fibrinogen gamma chain, leucine-rich alpha-2-glycoprotein, haptoglobin and apolipoprotein A–I) are shown as 3-D images as well as the associated graph views of standardized abundances of the selected spots and spot locations (Fig. 5).

3.2. Validation by immunoblotting and ELISA

To verify the abundances of proteins deduced from the results of 2D-DIGE and MALDI–TOF MS, the abundance levels of identified RSK2, leucine-rich alpha-2-glycoprotein, hapatoglobin, vitamin D-binding protein, hemopexin were investigated by immunoblotting and ELISA. As is shown in Fig. 6A and B, the 84 kDa of RSK2, 38 kDa of leucine-rich alpha-2-glycoprotein and the 46 kDa of hapatoglobin were significantly increased in the plasma of patients with OSCC. Additionally, an ELISA assay was also performed to verify proteomic results (Fig. 6C). There were significant increases in the level of haptoglobin and leucine-rich alpha-2-glycoprotein in the OSCC patients as compared to the healthy donors. In contrast, the level of hemopexin and vitamin D-binding protein were significantly lower in OSCC plasma (Figure 6A, B and C). These immunoblotting and ELISA results are consistent with the data from the 2D-DIGE and MALDI–TOF MS, and further suggest that the identified proteins may be employed as potential markers for the early diagnosis of OSCC.

4. Conclusion

The quantitative plasma proteomics analysis based on 2D-DIGE and MALDI–TOF MS provided a valuable impact for OSCC research. The current quantitative proteomic approach has identified vitamin D-binding protein which has been reported as a plasma marker of OSCC. Additionally, this study has presented several putative OSCC biomarkers including fibrinogen (alpha/beta/gamma) chain, haptoglobin, leucine-rich alpha-2-glycoprotein and RSK2, which may be associated with the progression and development of the disease and has a potential to serve as a useful tool for monitoring the course of the disease. The potential of utilizing these markers for screening and treating OSCC warrants further investigation.

Acknowledgments

This work was supported by NSC grant (100–2311-B-007–005) from National Science Council, Taiwan, Nano- and Micro-ElectroMechanical Systems-based Frontier Research on Cancer Mechanism, Diagnosis, and Treatment grant from National Tsing Hua University. The authors also thank the grant (Ditmanson Medical Foundation Chia-Yi Christian Hospital Research Program; R101-8) supported from the Chiayi Christian Hospital, Chiayi, Taiwan.

References

[1] Y.S. Lin, Y.M. Jen, B.B. Wang, J.C. Lee, B.H. Kang, Epidemiology of oral cavity cancer in Taiwan with emphasis on the role of betel nut chewing, ORL J. Otorhinolaryngol. Relat Spec. 67 (2005) 230–236.
[2] J.M. Carpenter, M.J. Syms, J.C. Sniezek, Oral carcinoma associated with betel nut chewing in the pacific: an impending crisis? Pac. Health Dialog. 12 (2005) 158–162.
[3] H.C. Lee, P.H. Yin, T.N. Yu, Y.D. Chang, W.C. Hsu, S.Y. Kao, C.W. Chi, T.Y. Liu, Y.H. Wei, Accumulation of mitochondrial DNA deletions in human oral tissues – effects of betel quid chewing and oral cancer, Mutat. Res. 493 (2001) 67–74.
[4] P.H. Chen, T.Y. Shieh, P.S. Ho, C.C. Tsai, Y.H. Yang, Y.C. Lin, M.S. Ko, P.C. Tsai, S.L. Chiang, H.P. Tu, Y.C. Ko, Prognostic factors associated with the survival of oral and pharyngeal carcinoma in Taiwan, BMC Cancer 7 (2007) 101.
[5] S.T. Lin, H.C. Chou, S.J. Chang, Y.W. Chen, P.C. Lyu, W.C. Wang, M.D. Chang, H.L. Chan, Proteomic analysis of proteins responsible for the development of doxorubicin resistance in human uterine cancer cells, J. Proteomics 75 (2012) 5822–5847.
[6] C.L. Wu, H.C. Chou, C.S. Cheng, J.M. Li, S.T. Lin, Y.W. Chen, H.L. Chan, Proteomic analysis of UVB-induced protein expression- and redox-dependent changes in skin fibroblasts using lysine- and cysteine-labeling two-dimensional difference gel electrophoresis, J. Proteomics 75 (2012) 1991–2014.
[7] C.H. Lai, N.W. Chang, C.F. Lin, C.D. Lin, Y.J. Lin, L. Wan, J.J. Sheu, S.Y. Chen, Y.P. Huang, Y.T. Sing, T.W. Tao, C.K. Lai, M.H. Tsai, H.L. Chan, Y.J. Jou, C.W. Lin, Proteomics-based identification of haptoglobin as a novel plasma biomarker in oral squamous cell carcinoma, Clin. Chim. Acta 411 (2010) 984–991.
[8] Y.J. Jou, C.D. Lin, C.H. Lai, C.H. Chen, J.Y. Kao, S.Y. Chen, M.H. Tsai, S.H. Huang, C.W. Lin, Proteomic identification of salivary transferrin as a biomarker for early detection of oral cancer, Anal. Chim. Acta 681 (2010) 41–48.
[9] Y.W. Chen, J.Y. Liu, S.T. Lin, J.M. Li, S.H. Huang, J.Y. Chen, J.Y. Wu, C.C. Kuo, C.L. Wu, Y.C. Lu, Y.H. Chen, C.Y. Fan, P.C. Huang, C.H. Law, P.C. Lyu, H.C. Chou, H.L. Chan, Proteomic analysis of gemcitabine-induced drug resistance in pancreatic cancer cells, Mol. Biosyst. 7 (2011) 3065–3074.
[10] T.C. Lai, H.C. Chou, Y.W. Chen, T.R. Lee, H.T. Chan, H.H. Shen, W.T. Lee, S.T. Lin, Y.C. Lu, C.L. Wu, H.L. Chan, Secretomic and proteomic analysis of potential breast cancer markers by two-dimensional differential gel electrophoresis, J. Proteome. Res. 9 (2010) 1302–1322.
[11] P.H. Hung, Y.W. Chen, K.C. Cheng, H.C. Chou, P.C. Lyu, Y.C. Lu, Y.R. Lee, C.T. Wu, H.L. Chan, Plasma proteomic analysis of the critical limb ischemia markers in diabetic patients with hemodialysis, Mol. Biosyst. 7 (2011) 1990–1998.
[12] D.J. Rader, Regulation of reverse cholesterol transport and clinical implications, Am. J. Cardiol. 92 (2003) 42J–49J.
[13] P.K. Chong, H. Lee, J. Zhou, S.C. Liu, M.C. Loh, J.B. So, K.H. Lim, K.G. Yeoh, Y.P. Lim, Reduced plasma APOA1 level is associated with gastric tumor growth in MKN45 mouse xenograft model, J. Proteomics 73 (2010) 1632–1640.
[14] H. Takeuchi, S. Ikeuchi, Y. Kitagawa, A. Shimada, T. Oishi, Y. Isobe, K. Kubochi, M. Kitajima, S. Matsumoto, Pretreatment plasma fibrinogen level correlates with tumor progression and metastasis in patients with squamous cell carcinoma of the esophagus, J. Gastroenterol. Hepatol. 22 (2007) 2222–2227.

[15] J.D. Andersen, K.L. Boylan, R. Jemmerson, M.A. Geller, B. Misemer, K.M. Harrington, S. Weivoda, B.A. Witthuhn, P. Argenta, R.I. Vogel, A.P. Skubitz, Leucine-rich alpha-2-glycoprotein-1 is upregulated in sera and tumors of ovarian cancer patients, J. Ovarian. Res. 3 (2010) 21.
[16] S. Kang, J. Chen, Targeting RSK2 in human malignancies, Expert. Opin. Ther. Targets 15 (2011) 11–20.
[17] C.C. Chiu, B.H. Chen, T.C. Hour, W.F. Chiang, Y.J. Wu, C.Y. Chen, H.R. Chen, P.T. Chan, S.Y. Liu, J.Y. Chen, Betel quid extract promotes oral cancer cell migration by activating a muscarinic M4 receptor-mediated signaling cascade involving SFKs and ERK1/2, Biochem. Biophys. Res. Commun. 399 (2010) 60–65.
[18] J.Y. Chen, C.C. Hung, K.L. Huang, Y.T. Chen, S.Y. Liu, W.F. Chiang, H.R. Chen, C.Y. Yen, Y.J. Wu, J.Y. Ko, Y.S. Jou, Src family kinases mediate betel quid-induced oral cancer cell motility and could be a biomarker for early invasion in oral squamous cell carcinoma, Neoplasia 10 (2008) 1393–1401.
[19] S. Kang, S. Dong, A. Guo, H. Ruan, S. Lonial, H.J. Khoury, T.L. Gu, J. Chen, Epidermal growth factor stimulates RSK2 activation through activation of the MEK/ERK pathway and src-dependent tyrosine phosphorylation of RSK2 at Tyr-529, J. Biol. Chem. 283 (2008) 4652–4657.
[20] S. Elf, D. Blevins, L. Jin, T.W. Chung, I.R. Williams, B.H. Lee, J.X. Lin, W.J. Leonard, J. Taunton, H.J. Khoury, S. Kang, p90RSK2 is essential for FLT3-ITD- but dispensable for BCR-ABL-induced myeloid leukemia, Blood 117 (2011) 6885–6894.
[21] D.E. Clark, T.M. Errington, J.A. Smith, H.F. Frierson Jr., M.J. Weber, D.A. Lannigan, The serine/threonine protein kinase, p90 ribosomal S6 kinase, is an important regulator of prostate cancer cell proliferation, Cancer Res. 65 (2005) 3108–3116.
[22] K. Bijian, A.M. Mlynarek, R.L. Balys, S. Jie, Y. Xu, M.P. Hier, M.J. Black, M.R. Di Falco, S. LaBoissiere, M.A. Alaoui-Jamali, Serum proteomic approach for the identification of serum biomarkers contributed by oral squamous cell carcinoma and host tissue microenvironment, J. Proteome Res. 8 (2009) 2173–2185.
[23] K. Bijian, A.M. Mlynarek, R.L. Balys, S. Jie, Y. Xu, M.P. Hier, M.J. Black, M.R. Di Falco, S. LaBoissiere, M.A. Alaoui-Jamali, Serum proteomic approach for the identification of serum biomarkers contributed by oral squamous cell carcinoma and host tissue microenvironment, J. Proteome Res. 8 (2009) 2173–2185.
[24] H.L. Chan, S. Gharbi, P.R. Gaffney, R. Cramer, M.D. Waterfield, J.F. Timms, Proteomic analysis of redox- and ErbB2-dependent changes in mammary luminal epithelial cells using cysteine- and lysine-labelling two-dimensional difference gel electrophoresis, Proteomics 5 (2005) 2908–2926.
[25] D.S. Dalpathado, H. Desaire, Glycopeptide analysis by mass spectrometry, Analyst 133 (2008) 731–738.
[26] T. Rabilloud, M. Heller, F. Gasnier, S. Luche, C. Rey, R. Aebersold, M. Benahmed, P. Louisot, J. Lunardi, Proteomics analysis of cellular response to oxidative stress. Evidence for in vivo overoxidation of peroxiredoxins at their active site, J. Biol. Chem. 277 (2002) 19396–19401.
[27] E. Wagner, S. Luche, L. Penna, M. Chevallet, A. van Dorsselaer, E. Leize-Wagner, T. Rabilloud, A method for detection of overoxidation of cysteines: peroxiredoxins are oxidized in vivo at the active-site cysteine during oxidative stress, Biochem. J. 366 (2002) 777–785.